

Guiding and nonlinear coupling of light in plasmonic nanosuspensions

TREVOR S. KELLY,¹ YU-XUAN REN,¹ AKBAR SAMADI,¹ ANNA BEZRYADINA,¹
DEMETRIOS CHRISTODOULIDES,² AND ZHIGANG CHEN^{1,3,*}

¹Department of Physics and Astronomy, San Francisco State University, San Francisco, California 94132, USA

²CREOL/College of Optics, University of Central Florida, Orlando, Florida 32816, USA

³TEDA Applied Physics Institute and School of Physics, Nankai University, Tianjin 300457, China

*Corresponding author: zhigang@sfsu.edu

Received 24 May 2016; revised 23 July 2016; accepted 24 July 2016; posted 25 July 2016 (Doc. ID 266537); published 9 August 2016

We demonstrate two different types of coupled beam propagation dynamics in colloidal gold nanosuspensions. In the first case, an infrared (IR) probe beam (1064 nm) is guided by a low-power visible beam (532 nm) in a gold nanosphere or in nanorod suspensions due to the formation of a plasmonic resonant soliton. Although the IR beam does not experience nonlinear self-action effects, even at high power levels, needle-like deep penetration of both beams through otherwise highly dissipative suspensions is realized. In the second case, a master/slave-type nonlinear coupling is observed in gold nanoshell suspensions, in which the nanoparticles have opposite polarizabilities at the visible and IR wavelengths. In this latter regime, both beams experience a self-focusing nonlinearity that can be fine-tuned. © 2016 Optical Society of America

OCIS codes: (190.6135) Spatial solitons; (250.5403) Plasmonics; (190.4720) Optical nonlinearities of condensed matter; (230.7370) Waveguides.

<http://dx.doi.org/10.1364/OL.41.003817>

The unique optical properties of artificial soft-matter systems have been the subject of extensive research since Ashkin's early pioneering work [1]. For example, colloidal suspensions containing dielectric micro- or nanoparticles have been shown to exhibit nontrivial nonlinearities that could lead to modulation instability and optical spatial solitons [2–12]. These nonlinearities can be understood to be a consequence of optical force-induced refractive index changes. In colloidal suspensions, the micro- or nanoparticles will be either attracted or repelled by a laser beam, depending on whether the sign of their optical polarizability is positive or negative, respectively [5,10]. Typically, suspended particles have a positive polarizability (PP), since they have a higher refractive index than the background solution, thus promoting enhanced scattering and a catastrophic beam collapse [5,8]. Recently, however, deep penetration of light through scattering dielectric nanosuspensions has been achieved through different mechanisms [9–12]. Furthermore, robust propagation of self-trapped light over

distances exceeding 25 diffraction lengths has been demonstrated in plasmonic nanosuspensions [13]. Guiding and steering light has also been observed in colloidal suspensions of dielectric (polystyrene), as well as metallic (silver) nanoparticles [14,15].

In this Letter, we show that self-induced waveguides can be established in colloidal nanosuspensions through the formation of plasmonic resonant solitons. The soliton-induced waveguides are typically 4 cm long and, in principle, can exceed those observed in organic glasses or nonlinear crystals [16,17]. We show that the wavelength-dependent optical nonlinearity in a plasmonic nanosuspension can be exploited in such a way so that linear guidance of a strong infrared (IR) optical beam (as a “probe”) can be achieved through a weak visible soliton-forming beam (used as a “pump”). The guided IR output pattern depends on the input power of the self-trapping beam. Furthermore, in gold nanoshell suspensions, a master/slave-type nonlinear coupling is observed in which both the probe and pump beams contribute to the self-focusing nonlinearity.

The setup used for these experiments is illustrated in Fig. 1, where a continuous-wave (CW) laser operating at $\lambda = 532$ nm (green) is used as the pump, while another CW laser operating at an IR wavelength ($\lambda = 1064$ nm) is used as the probe. Both beams propagate collinearly through a 4 cm long cuvette containing different nanoparticle (gold nanosphere, nanorod,

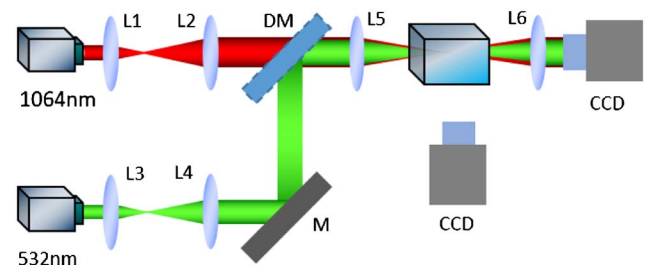


Fig. 1. Schematic of the experimental setup. An IR beam (as a probe) is combined with a green beam (as a pump), propagating collinearly through a sample (a 4 cm cuvette containing a nanosuspension). The images of input/output transverse intensity patterns and the side view of the beam propagation are taken by CCDs.

or nanoshell) suspensions. The green beam passes through a half-wave plate and polarizing beam splitter (not shown in Fig. 1) so that its power can be adjusted, and it is expanded/collimated before being focused near the input facet of the sample. The IR beam is also expanded/collimated and is combined with the green beam through a dichroic mirror before being focused together by a lens with a focal length of 80 mm. The diameters of the collimated green and IR beams are 5.0 and 6.5 cm, respectively, and the corresponding beam sizes at the focal plane are measured to be 21.4 and 16.6 μm . The beam propagation through the sample is monitored with different cameras. The side views of the visible light beam are taken with a regular Canon camera, while those of the IR beam are taken using a CCD camera (Thorlabs, USB 2.0), together with a Zeiss microscope eyepiece for magnification. Another CCD camera (Coherent, USB 2.0) assisted with a BeamView imaging system is used to record the input/output beam profiles before and after the cuvette. Due to the long sample and the two wavelengths used, the imaging system is slightly adjusted for each experiment to ensure that the camera can image the desired locations through the sample for both wavelengths.

The green pump beam can create self-trapped channels in nanoparticle suspensions through the formation of plasmonic resonant solitons [13]. Specifically, the optical gradient force on a suspended particle is not only intensity dependent, but also dependent on the polarizability of a particular nanosuspension. The sign of the polarizability is determined by the relative index of refraction between the particles and the background medium. As such, particles with PP in the suspension are pulled into the path of the laser beam, whereas particles with negative polarizability (NP) in the suspension are repelled by the beam. In either case, the light-particle interaction leads to a nonlinear optical response because of an increase in the refractive index along the beam path that leads to self-focusing. This self-focusing nonlinearity allows a beam to penetrate a long colloidal suspension of nanoparticles that would have been otherwise impossible because of diffraction, diffusion, and scattering [10,13]. In the following paragraphs, we focus on linear guiding and nonlinear coupling of optical beams in such nanosuspensions.

Our first guiding experiment is conducted in an aqueous suspension containing gold nanospheres with an average diameter of 40 nm [Fig. 2(a)]. The “pump” or soliton-forming beam is focused inside, but near the front facet of the cuvette. As the power for the green beam is increased gradually, a self-trapped channel is formed at an output power of only 60 mW, as seen by the side view of the soliton beam [Fig. 2(b)]. According to theoretical calculations [13], the gold nanospheres in the suspension are positively polarized at 532 nm, experiencing low scattering, but strong, absorption at this wavelength. Particles are attracted along the beam path, which leads to self-trapping of the beam without a beam collapse at lower power levels. This is attributed to a combined action of optical force-induced self-focusing nonlinearity and self-defocusing thermal effects, which gives rise to a cubic-quintic nonlinear response in the colloidal suspension [13,15].

When an IR probe beam is launched into the same nanosphere suspension (without the green soliton beam), it does not experience appreciable nonlinear self-action, even when its power is increased to 500 mW. Instead, the IR beam tends

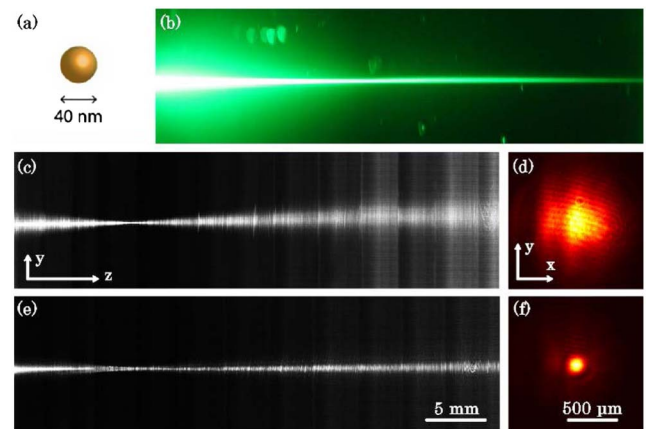


Fig. 2. Guiding an IR beam by a green soliton beam in a colloidal suspension of gold nanospheres. (a) Illustration of a gold nanosphere. (b) Side view of the soliton beam. (c), (d) Side view and transverse output pattern of the IR probe beam in the linear diffraction regime when the soliton beam is absent. (e), (f) Corresponding results when the soliton beam is present. (The IR side-view pictures were composed of hundreds of superimposed images due to weak scattering at the IR wavelength.)

to diffract in the suspension, as shown from the side view [Fig. 2(c)] and the cross-sectional output [Fig. 2(d)]. However, once the green soliton beam is switched on, the IR beam is guided and is well confined in the soliton-induced waveguide [Figs. 2(e) and 2(f)]. For the results obtained in Fig. 2, the power of the probe beam is about 50 mW. Linear diffraction of an IR probe beam (with the soliton beam off) and guidance (with the soliton beam on) is observed for a wide range (20–500 mW) of input power, although more pronounced guidance is realized at a low power as opposed to a high power. It should be pointed out that the 1064 nm wavelength is far away from the plasmonic resonance of the

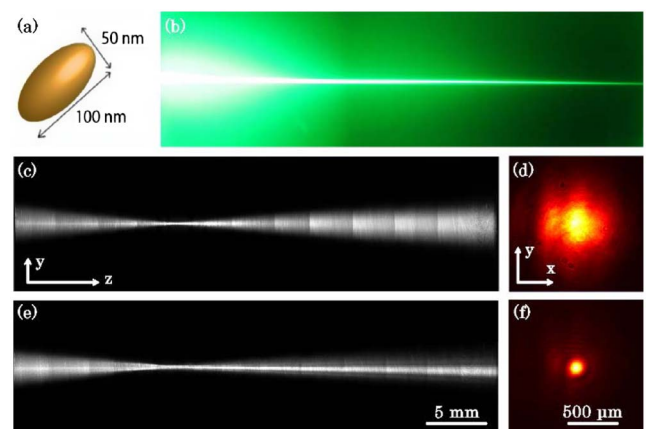


Fig. 3. Guiding an IR probe beam by a green soliton beam in a colloidal suspension of gold nanorods. (a) Illustration of a gold nanorod. (b) Side view of the soliton beam. (c), (d) Side view and transverse output pattern of the IR probe beam in the linear diffraction regime when the soliton beam is absent. (e), (f) Corresponding results when the soliton beam is present. (The IR side-view pictures were composed of hundreds of superimposed images due to weak scattering at the IR wavelength.)

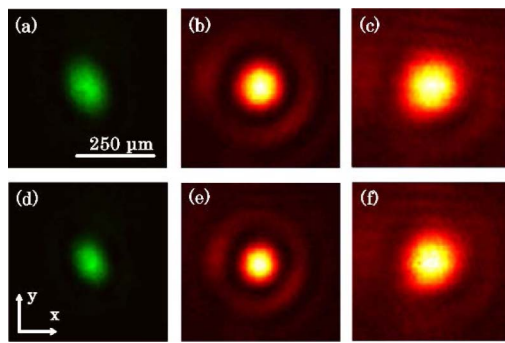


Fig. 4. Transverse output patterns of the (a), (d) self-trapped green pump beam and (b), (c), (e), (f) the guided IR probe beam at different pump beam powers. (a)–(c) For gold nanospheres when the green beam power is decreased from (b) 60 to (c) 30 mW. (d)–(f) For gold nanorods when the green beam power is decreased from (e) 100 to (f) 40 mW. The power of the probe beam is kept at 50 mW.

gold nanosphere and, hence, is subjected to very weak absorption and scattering [13]. In fact, since our camera is not very sensitive to IR light and the scattering from the IR beam is so weak, we had to develop a scheme (by combining integration and scanning) to construct the side-view images shown in Figs. 2(c) and 2(e). This was achieved by taking a short movie at different sections across the sample length and then superimposing all image frames (up to 2000 frames for a movie of 4 min) taken from the scattered light for each section to reconstruct the side view of the probe beam across the entire sample.

We then performed similar experiments in a colloidal suspension of gold nanorods. The gold nanorods employed for our experiment have an average diameter of 50 nm and a length of 100 nm [Fig. 3(a)]. Analysis suggests that [13] the polarizability for an aqueous suspension of such gold nanorods is negative at 532 nm. Nevertheless, since the particles are effectively pushed away from the beam center, nonlinear self-focusing still occurs [10,13]. Figure 3(b) shows a typical experimental result of a self-trapped channel of the green beam observed at a power

of 100 mW. On the other hand, the IR beam alone again undergoes normal diffraction, even when its power is increased to ~ 1 W. As shown in Figs. 3(c) and 3(d), the IR beam itself displays no nonlinear self-action at a power of 50 mW. However, when the green soliton beam is turned on, the guidance of the IR beam into the soliton-induced waveguide channel is reestablished [Figs. 3(e) and 3(f)].

Thus, even though the colloidal gold nanospheres and nanorods have different polarizability signs at 532 nm, linear guidance of the IR beam can be observed in both suspensions. This confirms that, in both PP and NP suspensions, optical force-induced nonlinearity can elevate the refractive index, thus establishing a waveguide along the beam path, which guides not only the soliton beam, but also another beam at a wavelength far off plasmonic resonance.

Although the IR beam by itself is not capable of forming a self-trapped channel, and its confinement in these nanosuspensions is mainly due to the guidance provided by the green soliton-induced waveguide, the presence of the IR probe beam slightly changes the output patterns of both beams. This can be seen from the guided output pattern of the probe beam that directly depends on the input power of the self-trapped green beam. As seen in Fig. 4, after the green beam is self-trapped (at 60 mW for the gold nanosphere [Fig. 4(a)] and 100 mW for nanorod suspensions [Fig. 4(d)]), it becomes less focused when the probe is sent through, unless the soliton beam power is reduced. The change in the guided output patterns of the probe beam due to a reduction of the soliton beam power is shown in the second and third columns of Fig. 4. Our results indicate that, after introducing the probe beam, the power of the pump beam needs to be reduced to maintain a well self-trapped channel. While the dynamics of this beam interaction need to be explored further, this suggests that the IR beam, although far away from the plasmonic resonance, could introduce a weak nonlinearity.

Finally, we demonstrated a master/slave vector-type nonlinear coupling between the two beams mentioned above. The nonlinear coupling was accomplished in silica-gold core-shell nanosuspensions, since both the green and IR beams can exhibit appreciable nonlinearities. The nanoshell particles have

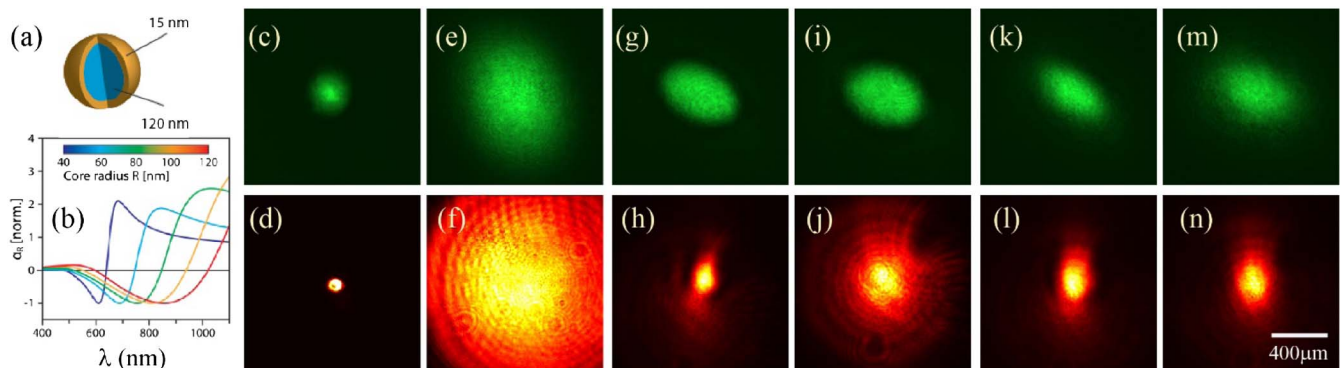


Fig. 5. Nonlinear coupling of a green beam (top) and an IR beam (bottom) in the colloidal suspensions of gold nanoshells. (a) Illustration of a core-shell nanoparticle with a silica-core diameter of 120 nm and a gold-shell thickness of 15 nm. (b) Plot of calculated polarizability vs. wavelength for different particle sizes. [13] (c), (d) Transverse intensity patterns of focused input beams. (e), (f) Linear diffraction output after 4 cm of propagation through the nanosuspension. (g), (h) Nonlinear coupled output when the green beam has a dominant nonlinearity, so the green beam remains self-trapped, but the IR beam exhibits only partial focusing after being decoupled, i.e., when the other coupling beam is removed (i), (j). (k)–(n) Similar to (g)–(j), except that the IR beam has a dominant nonlinearity.

an average silica-core radius of 60 nm and a gold-shell thickness of 15 nm [Fig. 5(a)]. The nanoshells in an aqueous suspension exhibit an NP at 532 nm, but a PP at 1064 nm, as seen from the light blue curve in the theoretical calculation [13] shown in Fig. 5(b). In such a soft-matter environment, we observe a tunable nonlinear coupling between the two beams by varying the relative strength of nonlinearities due to the competing PP and NP effects exhibited at 1064 and 532 nm, respectively. At appropriate low intensities, both beams are unable to create self-trapped channels alone; yet, they achieve mutual self-trapping when both are present (coupled). At the coupled regime with one beam dominant, the dominant beam exhibits a nonlinearity higher than that of the pairing beam, resulting in the self-focusing abilities being less affected after removal of the pairing beam (decoupled). Typical experimental results are shown in Fig. 5. The coupling and decoupling scheme is similar to that used for an earlier demonstration of a coupled soliton pair or vector soliton [18]. Figures 5(c)–5(f) show the beam patterns near the focal point and their linear diffraction after 4 cm of propagation through the suspension. Figures 5(g)–5(j) show this nonlinear coupling when both the green and IR beams are present and undergo nonlinear self-focusing, but the green beam dominates (i.e., exhibits a higher nonlinearity). This can be seen since the green beam is affected less after removing its partner beam (decoupled). Likewise, when the IR beam dominates [Figs. 5(k)–5(n)], the green beam experiences less self-focusing when it is decoupled from the IR beam, whereas the IR beam does not show significant change when the green beam is blocked. It should be pointed out that a perfect balance of the nonlinear action between the two beams is difficult to reach in an experiment.

In conclusion, we have observed the guiding of an IR light beam in a self-trapped green beam in a plasmonic nanosuspension composed of either gold spheres or rods. We have also demonstrated nonlinear coupling of two beams in gold nanoshell suspensions. The fact that a weak visible beam can guide an intense invisible beam in a variety of colloidal suspensions could be of interest and may bring about new possibilities for applications in optical manipulation, as well as optofluidics and biophotonics.

Funding. National Science Foundation (NSF) (PHY-1404510, DMR-1420620); National Institutes of Health (NIH) (1R15GM112117-01); Army Research Office (ARO) (W911NF-15-1-0413).

Acknowledgment. The authors thank R. Bland, S. Fardad, and A. Salandrino for their assistance.

REFERENCES

1. A. Ashkin, J. M. Dziedzic, and P. W. Smith, *Opt. Lett.* **7**, 276 (1982).
2. Z. Chen, M. Segev, and D. N. Christodoulides, *Rep. Prog. Phys.* **75**, 086401 (2012).
3. C. Conti, G. Ruocco, and S. Trillo, *Phys. Rev. Lett.* **95**, 183902 (2005).
4. P. J. Reece, E. M. Wright, and K. Dholakia, *Phys. Rev. Lett.* **98**, 203902 (2007).
5. R. El-Ganainy, D. N. Christodoulides, C. Rotschild, and M. Segev, *Opt. Express* **15**, 10207 (2007).
6. M. Matuszewski, W. Krolikowski, and Y. S. Kivshar, *Opt. Express* **16**, 1371 (2008).
7. W. M. Lee, R. El-Ganainy, D. N. Christodoulides, K. Dholakia, and E. M. Wright, *Opt. Express* **17**, 10277 (2009).
8. R. El-Ganainy, D. N. Christodoulides, E. M. Wright, W. M. Lee, and K. Dholakia, *Phys. Rev. A* **80**, 053805 (2009).
9. C. Conti and E. DelRe, *Phys. Rev. Lett.* **105**, 118301 (2010).
10. W. Man, S. Fardad, Z. Zhang, J. Prakash, M. Lau, P. Zhang, M. Heinrich, D. N. Christodoulides, and Z. Chen, *Phys. Rev. Lett.* **111**, 218302 (2013).
11. S. Fardad, M. S. Mills, P. Zhang, W. Man, Z. Chen, and D. N. Christodoulides, *Opt. Lett.* **38**, 3585 (2013).
12. E. Greenfield, J. Nemirovsky, R. El-Ganainy, D. N. Christodoulides, and M. Segev, *Opt. Express* **21**, 23785 (2013).
13. S. Fardad, A. Salandrino, M. Heinrich, P. Zhang, Z. Chen, and D. N. Christodoulides, *Nano Lett.* **14**, 2498 (2014).
14. R. A. Terborg, J. P. Torres, and K. Volke-Sepulveda, *Opt. Lett.* **38**, 5284 (2013).
15. A. S. Reyna and C. B. de Araújo, *Opt. Lett.* **41**, 191 (2016).
16. M. Shih, Z. Chen, M. Mitchell, and M. Segev, *J. Opt. Soc. Am. B* **14**, 3091 (1997).
17. M. Asaro, M. Sheldon, Z. Chen, O. Ostroverkhova, and W. E. Moerner, *Opt. Lett.* **30**, 519 (2005).
18. Z. Chen, M. Segev, T. H. Coskun, and D. N. Christodoulides, *Opt. Lett.* **21**, 1436 (1996).